Isotropic tensile strength of molecular glasses

Marcel Utz[a) and Pablo G. Debenedetti
Department of Chemical Engineering, Princeton University, Princeton New Jersey 08544

Frank H. Stillinger
Princeton Materials Institute, Princeton University, Princeton New Jersey 08544 and Bell Laboratories, Lucent Technologies, Murray Hill, New Jersey 07974

The relationship between the bulk density and pressure of configurations corresponding to local minima on the potential energy surface of molecular models of ethane, n-pentane, and cyclopentane (the equation of state of their energy landscape) has been explored. Like simpler, atomic fluids, these systems exhibit a limiting bulk density below which minimum energy configurations are no longer spatially homogeneous, but consist instead of a locally dense fraction and large, system-spanning voids. In the case of n-pentane, the sampling of the minima on the energy landscape was found to depend strongly on temperature, due to changing Boltzmann factors associated with the different conformers in the liquid. The pressures of the minimum energy configurations, in contrast, were found to be essentially independent of the liquid temperature in all cases. The highest amount of isotropic tension (negative pressure) that minimum energy configurations can sustain is reached at the limiting densities, and is of similar magnitude (approximately 250 MPa) for all three model substances. Crystalline configurations of ethane and n-pentane, in contrast, were found to exhibit higher isotropic tensile strength than their amorphous counterparts. A pronounced segregation of end groups on the boundary of large voids was observed in the minimum energy configurations of low bulk density pentane. © *2001 American Institute of Physics.* [DOI: 10.1063/1.1370958]

I. INTRODUCTION

Understanding the physical nature of the glassy state of matter, as well as the transition which separates it from the liquid, still presents a challenge to materials science. The potential energy as a function of the system's degrees of freedom (energy landscape) provides a useful framework to describe and understand the dynamics of glass-forming liquids[1] as well as the glass transition.[2] Sastry *et al.*[3] have recently reported a detailed study of the energy landscape of atomic fluids as a function of density. Their key finding was a limiting density ρ_S, below which spatially homogeneous inherent structures (local minima of the potential energy hypersurface) no longer exist. Rather, the inherent structures exhibit regions of vanishing density (voids), which grow as the overall density decreases.[4] This pattern was first observed by LaViolette.[5] At low enough bulk densities, the inherent structures are in a state of tension (negative pressure), and the limiting density coincides with the maximum tension that the amorphous system can sustain.[6] The inherent structure pressure P_{IS} as a function of density ρ represents an ''equation of state'' of the local minima on the energy landscape.[7]

According to the thermodynamic viewpoint, the laboratory glass transition can be interpreted as the kinetically controlled manifestation of an underlying phase transition associated with the vanishing of the configurational entropy of the supercooled liquid as temperature decreases.[8–10] From this perspective, the existence of a limiting density, below which homogeneous inherent structures, and hence homogeneous glasses no longer exist, is particularly interesting, and may lead to a more fundamental understanding of the glass transition in general. This is because this density appears to be an absolute (thermodynamic) bound to vitrification, in the limit of very low temperatures.[7] Were this to be the case, a low-temperature convergence between the superheated liquid spinodal and the Kauzmann locus (along which the difference in entropy between a supercooled liquid and its stable crystalline form vanishes at a given pressure) would exist.[7] Recent mean-field calculations have indeed shown such a convergence.[7] It is therefore important to clarify whether the behavior reported by Sastry *et al.* for atomic liquids can be found in other, more complex classes of materials, such as molecular fluids, ionic liquids, and polymers.

So far, the equation of state of the energy landscape has only been studied for atomic liquids[3] and for the SPC/E model of water.[11] The inherent structure energy and pressure of single-component atomic fluids have been found to be essentially independent of the temperature of the liquid.[4] In contrast, a more complex behavior was found in the case of water: at fixed density, the directional hydrogen bonds cause the liquid to sample different inherent structures as a function of its temperature, and, as a consequence, both the inherent structure energy and pressure become temperature dependent.[11]

In this paper we report the initial results of an analogous investigation of the temperature and density dependence of

---

[a)Current address: Institute of Materials Science and Department of Physics, University of Connecticut, Storrs, CT 06269. Electronic mail: marcel.utz@uconn.edu

10049

TABLE I. Parameters of the Lennard-Jones interaction between CH_3 and CH_2 pseudoatoms used in the present models of aliphatic hydrocarbons.

| | ϵ[J/mol] | | σ[Å] | |
	CH_2	CH_3	CH_2	CH_3
CH_2	414.2		3.93	
CH_3	645.1	1004.4	3.93	3.93

the energy and pressure of inherent structures in molecular liquids. In particular, we study the linear and cyclic hydrocarbons ethane, n-pentane, and cyclopentane. Molecular and atomic liquids differ in two important aspects: On the one hand, molecules are not spherically symmetric, which can give rise to complex packing behavior. On the other hand, many molecules are flexible, which introduces additional internal degrees of freedom into the energy landscape. The present study aims at exploring both aspects by studying the inherent structures of simple molecular models. As a compromise between simplicity of the model and realism, we use the united atom potentials developed by Siepmann and co-workers for aliphatic hydrocarbons.[12,13] In order to study packing and conformational effects, we investigate the stiff, but nonspherical molecules ethane and cyclopentane, and the conformationally flexible n-pentane.

The model and the simulation method are described in Sec. II. Section III reports the equation of state of the energy landscape of ethane, n-pentane, and cyclopentane, and explores their microscopic structural bases (e.g., packing, conformations). In addition, results comparing the properties of amorphous structures inherent to crystalline systems, as well as findings concerning the role of end groups in forming internal voids in n-pentane, are reported. Finally, the main conclusions, and the implications of the present calculations for the physics of molecular glasses are presented in Sec. IV.

II. MODEL AND SIMULATION METHOD

The present simulations are based on the united-atom potentials for aliphatic hydrocarbons developed by Smit et al.[12,13] The parameters of this potential have been tuned to represent the phase behavior of linear and branched alkanes in Gibbs-ensemble Monte Carlo simulations. The force field is based on two different pseudoatom types, representing methyl (CH_3) and methylene (CH_2) groups, which interact through a two-body potential of the form

$$u^{nb}(r) = \begin{cases} 4\varepsilon\left[\left(\dfrac{\sigma}{r}\right)^{12} - \left(\dfrac{\sigma}{r}\right)^{6}\right] + cr^2 + d, & r < r_c \\ 0, & r \geq r_c, \end{cases} \quad (1)$$

with the Lennard-Jones interaction parameters σ and ε given in Table I. The cutoff length r_c was set to 9.75 Å, and the parameters c and d were chosen to make the potential continuously differentiable at the cutoff distance. This is required for the energy minimization step in the inherent structure calculation as well as for the molecular dynamics equilibration and deviates slightly from the force field used by Smit et al.,[12,13] in which the last two terms in Eq. (1) were absent. ε was increased by 6% over the values used by Smit

et al. to make the well depths of the two potentials the same. The usual tail corrections to the pressure and energy were applied.[14]

Interactions between bonded atoms include the following terms: the bond-angle potential is given by

$$u^{ang}(\theta) = k_\theta(\theta - \theta_0)^2, \quad (2)$$

with the constants $\theta_0 = 114°$ and $k_\theta = 158.29$ J/mol deg^2. The dihedral angle potential has the form

$$u^{tors}(\phi) = \sum c_k \cos^k(\phi), \quad (3)$$

with the constants $c_1 = 8.39$ kJ/mol, $c_2 = 0.57$ kJ/mol, and $c_3 = -13.16$ kJ/mol.[12] In contrast to the work by Smit et al., who used a fixed bond length in their Monte Carlo simulations, a flexible C–C bond with a harmonic potential

$$u^{bond}(l) = k_l(l - l_0)^2, \quad (4)$$

was applied in the present work. An equilibrium bond length of $l_0 = 1.53$ Å was used in conjunction with a spring constant $k_l = 345.8$ kJ/mol Å^2. This value is lower by about a factor of 5 compared to a realistic spring constant tuned to give correct IR and Raman frequencies.[15] At the low temperatures of interest in this study, only very small deviations from the equilibrium bond length occur even with this softened bond potential, and the softening is therefore inconsequential for the results derived here. However, it allows for a significantly larger time step in the molecular dynamics integration.[15]

In order to calculate the equation of state of the inherent structures of ethane, n-pentane, and cyclopentane, initial structures containing 686, 112, and 125 molecules, respectively, on an artificial regular grid (unrelated to the experimental crystal structures) have been subjected to 200 ps of NVT molecular dynamics[14] at $T = 1000$ K. During this equilibration step, temperature was held constant by rescaling the velocities of all particles every 0.5 ps. In order to generate starting configurations at high densities, the systems were then subjected to NPT Monte Carlo simulation at a pressure of $P = 1$ GPa and at temperatures of 300, 200, and 100 K. Each of the structures obtained under the protocol described above was then subjected to an NVT molecular dynamics run of 3.6 ns total length. Every 120 ps, the density of the system was reduced by approximately 3% by increasing the edge length of the simulation box by 1% while keeping the fractional coordinates of all particles fixed. Every 3 ps, inherent structures were obtained by conjugent gradient minimization of the potential energy,[16] and the inherent structure energy and pressure, as well as structural information, were saved to disk. In summary, this simulation protocol produced, for each of the three molecules studied, 40 different inherent structures at each of 30 different densities. In order to study the influence of the equilibration temperature, simulation runs have been performed at three different values $T_{equil} = 100$, 200, and 300 K.

An additional run of n-pentane at an equilibration temperature of $T = 300$ K, using an eightfold larger simulation cell (896 molecules), yielded inherent structure energies and pressures indistinguishable from the ones obtained at smaller
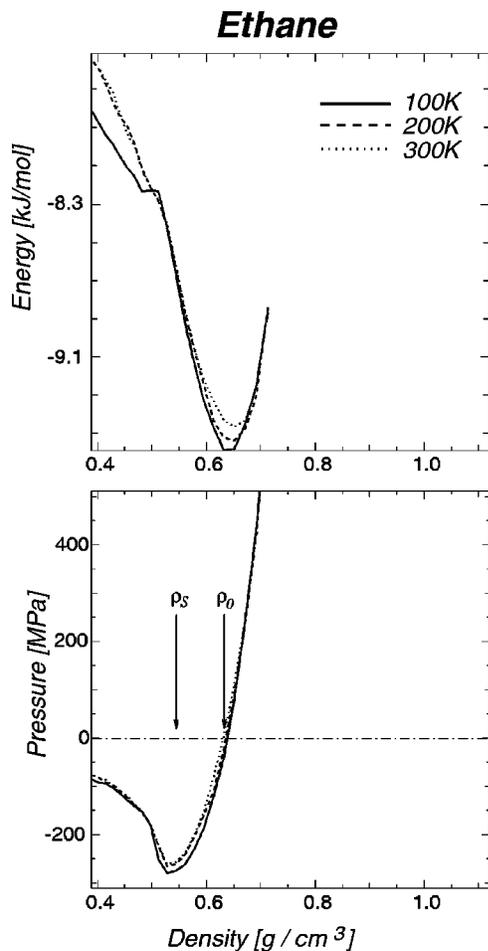
FIG. 1. Potential energy (top) and pressure (bottom) of inherent structures obtained from liquid ethane at various temperatures as a function of density. ρ_S (Sastry density) is the limit of mechanical stability of the inherent structures with respect to isotropic tension; ρ_0 corresponds to the minimum inherent structure energy and fulfills a zero-pressure condition.

FIG. 2. Potential energy (top) and pressure (bottom) of inherent structures obtained from liquid pentane at various temperatures as a function of density. ρ_S (Sastry density) is the limit of mechanical stability of the inherent structures with respect to isotropic tension; ρ_0 corresponds to the minimum inherent structure energy and fulfills a zero-pressure condition.

system sizes. We therefore conclude that the results reported in the following are not significantly influenced by finite-size effects.

III. RESULTS AND DISCUSSION

A. Inherent structures

The inherent structure energies and pressures of ethane, n-pentane, and cyclopentane are shown in Figs. 1, 2, and 3, respectively. In some sense, the function $P_{IS}(\rho)$ shown in the bottom panels of Figs. 1–3 is a zero-temperature isotherm, although points at neighboring densities along the curve are not directly connected by an isothermal path. Rather, the density is changed in the *liquid* state, at the equilibration temperature T_{equil}. The function $P_{IS}(\rho)$ has been called the ''equation of state'' of the energy landscape of the respective fluid.[7]

The curves show features that have already been observed in atomic liquids: below a density ρ_0, the inherent structures are under tension (negative pressure), which increases in magnitude as the density is lowered further. Note that ρ_0 corresponds to the minimum of the potential energy function $E(\rho)$. The extremal point ρ_S in the pressure curve

designates the largest isotropic tension that an amorphous solid prepared by quenching from the liquid can sustain. This limiting tension can also be called the ''isotropic tensile strength'' of the system. As the density falls below ρ_S, the inherent structures are no longer homogeneous, but contain an increasing fraction of empty space in the form of large, system-spanning voids.[4] The limiting density ρ_S is an important material property and is called the Sastry density.

Visual examination of the fractured inherent structures shows clearly that void space is irregular, multiply connected, and pervades the system volume. In this respect it is unlike the regular and simply connected volume of a vapor bubble (of macroscopic size if the system is itself macroscopic) that would be present in an equilibrium state of liquid–vapor coexistence.

In the case of single-component atomic liquids, no dependence of the equation of state of the inherent structure on the equilibration temperature was found.[4] An important objective of the present work is to find out if and to what extent deviations from spherical symmetry and the presence of internal degrees of freedom lead to complex (temperature-dependent) behavior.

FIG. 3. Potential energy (top) and pressure (bottom) of inherent structures obtained from liquid cyclopentane at various temperatures as a function of density. ρ_S (Sastry density) is the limit of mechanical stability of the inherent structures with respect to isotropic tension; ρ_0 corresponds to the minimum inherent structure energy and fulfills a zero-pressure condition.

TABLE II. Relationship between the calculated limiting densities and pressures (ρ_S,P_S) to critical parameters obtained from experiment and simulation.

| | Experimental CP data | | Simulation CP data | | Peng–Robinson[a] | |
	ρ_S/ρ_c	P_S/P_c	ρ_S/ρ_c	P_S/P_c	ρ_S/ρ_c	P_S/P_c
Ethane	2.61	−55			3.65	−87
n-Pentane	2.96	−80	3.08	−70	3.48	−110
c-Pentane	2.90	−67			3.18	−105

[a]Peng–Robinson predictions for both limiting (ρ_S,P_S) and critical (ρ_c,P_c) quantities.

into theoretical perspective by comparison with the critical parameters P_c and ρ_c. This is because the point (P_S,ρ_S) corresponds to the $T \rightarrow 0$ limit of the spinodal curve for the superheated liquid[3,7] which, in mean-field theories, bears a simple relationship with the critical density and pressure. Using experimental critical parameters, one finds the results shown in Table II. The model critical parameters have been determined by Smit *et al.* for n-pentane;[12,13] the corresponding values are also included in Table II. The van der Waals equation of state predicts $\rho_S/\rho_c=3$ and $P_S/P_c=-27$,[7] the latter value being about a factor of 2 smaller in magnitude than the ones determined from our simulations. The Peng–Robinson equation of state[17] gives better agreement, but tends to overestimate P_S/P_c (last column of Table II).

The marked dependence of the inherent structure energy of n-pentane on T_{equil} is a result of temperature-induced changes in the distribution of dihedral angles in the liquid. Figure 4 shows a comparison of the dihedral angle distributions of n-pentane at different temperatures, in the liquid state and in the inherent structures obtained by steepest descent energy minimization. The *trans* conformation ($\phi=0$) dominates in the low temperature liquid, with a minor population of the *gauche* state ($\phi=\pm 120°$). With increasing temperature, the *trans/gauche* ratio decreases, as expected from the Boltzmann factors associated with the two states. Interestingly, the liquid *trans/gauche* ratio is *conserved* in the inherent structures. Energy minimization leads to a marked sharpening of the dihedral angle distributions, as shown in the bottom row of Fig. 4, but the steepest-descent minimization protocol seems to preclude transitions between the *gauche* and the *trans* state. The inherent structures therefore become dependent on the equilibration temperature. The complex behavior of n-pentane in terms of the potential energy can therefore be attributed to the conformational flexibility of its molecules. The dihedral angle distributions of cylcopentane (not shown) are, in contrast, quite independent of temperature even in the liquid state due to the strained geometry of the molecule, and a complexity effect similar to n-pentane therefore cannot occur.

It is interesting to note that complex behavior in $E_{IS}(\rho)$ does not necessarily lead to complexity in the equation of state of the inherent structures $P_{IS}(\rho)$. The spread between the $P_{IS}(\rho)$ curves obtained from liquids equilibrated at different temperatures is small and similar in all three cases studied here, even for n-pentane, where the dihedral angle distribution in the inherent structures is sensitive on the equilibration temperature. It appears that the equation of

As shown in Figs. 1–3, the inherent structure energy $E_{IS}(\rho)$ exhibits a pronounced dependence on the equilibration temperature for n-pentane, whereas the effect is much smaller for both ethane and cyclopentane. The differences are largest around ρ_0 in all three cases. At ρ_0, they amount to about 300 J/mol for n-pentane, compared to only about 100 J/mol for ethane and 50 J/mol for cyclopentane. Interestingly, the equations of state $P_{IS}(\rho)$ are almost independent of the equilibration temperature. Small differences are noticeable close to the Sastry density ρ_S, but they remain below 50 MPa. It is also remarkable that the isotropic tensile strengths $P_{IS}(\rho_S)$ of the three systems studied here are very similar in magnitude (250–300 MPa), although the densities ρ_S corresponding to the minima are quite different. It seems that $P_{IS}(\rho_S)$ is primarily influenced by the nonbonded interactions, which are similar in all three cases, rather than the shape and flexibility of the molecules. This is corroborated by the fact that equation of state complexity has been reported for the SPC/E model of water,[11] which has intermolecular interactions (charges, hydrogen bonds) quite different from the aliphatic molecules under study here.

The limiting tension P_S and Sastry density ρ_S can be put

FIG. 4. Dihedral angle distributions in simulations of *n*-pentane. Top row: liquid state at various temperatures; bottom row: inherent structures obtained from the liquids by steepest-descent energy minimization.

state of the energy landscape is primarily influenced by the nonbonded interactions, which are similar in all three cases under study here, and that the internal structure, flexibility, and shape of the molecules play only a secondary role.

As already mentioned above, pronounced complex behavior has been observed in the equation of state of the energy landscape of water.[11] It therefore seems that specific directional intermolecular interactions, which lead to a temperature-dependent network structure in the liquid and the inherent structures, are sufficient to cause a complex equation of state, while conformational flexibility of the molecules by itself is not.

B. Comparison to crystals

The crystal structures of ethane and n-pentane are known from x-ray crystallography.[18,19] Of course, the structure corresponding to the absolute potential energy minimum for the force field employed (i.e., the crystal structure of the model) does not necessarily agree with the crystal structure found in nature. Nevertheless, the experimental crystal data from single-crystal x-ray structure determinations of ethane[18] and n-pentane[19] were used here as a starting point to make a reasonable guess for the crystal structure of the model, in order to compare the equations of state of crystalline and amorphous inherent structures. Initially, united-atom model systems were generated using the experimental carbon atom
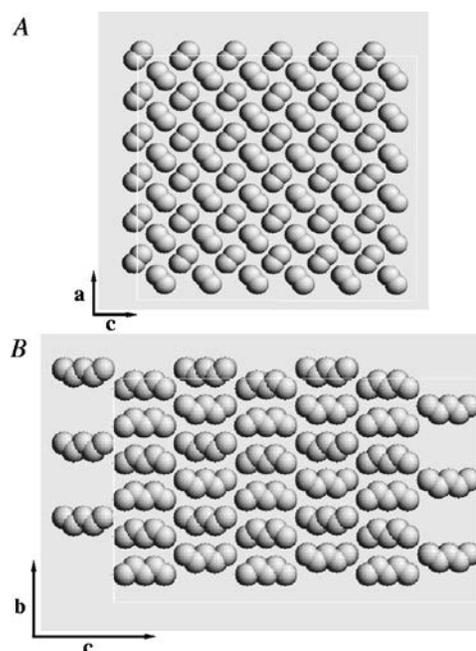
FIG. 5. United-atom crystal models of ethane (A) and n-pentane (Refs. 18 and 19). (B). The planes of projection are indicated in the figures.
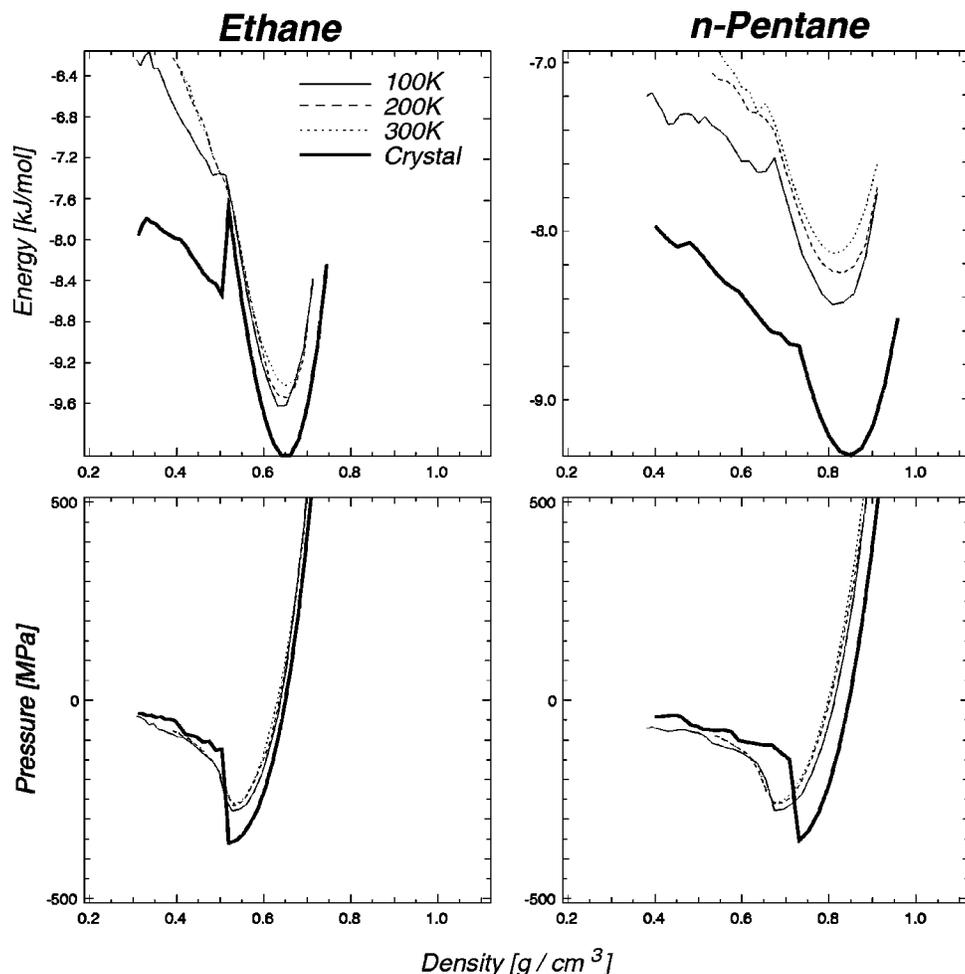
FIG. 6. Energies and pressures of ethane and n-pentane inherent structures obtained from the liquid at various temperatures (thin lines) in comparison with crystalline structures (bold solid lines).

positions as sites for the CH_2 and CH_3 pseudoatoms (Fig. 5). These systems were then relaxed by a variable-shape Monte Carlo simulation at zero stress at a temperature of 10 K. In both cases, this led to slight rearrangements in the crystal structure, together with an increase in symmetry: the space group of the ethane system changed from $P2_1/n$ to $P2_1/m$, that of n-pentane from $Pbcn$ to $Pbcm$. The absence of explicit hydrogen atoms from the force field leads to an increased symmetry of the ethane and n-pentane molecules. It is not surprising that this also manifests itself in a higher crystal symmetry. Since only the general aspects of the behavior of crystalline molecular solids are of interest here, the difference between the model crystal structures and the experimental ones are inconsequential for the conclusions drawn in this paper.

After relaxation at zero stress, the crystalline systems were subjected to a constant stress Monte Carlo run at an isotropic pressure of 1 GPa, followed by the same molecular dynamics / expansion protocol as the liquid samples. The only difference was the equilibration temperature in the MD run, which was chosen to be 10 K to prevent melting.

The results are shown in Fig. 6: the energies of the amorphous inherent structures lie above those for the crystalline ones in both cases and over the entire density range. The difference is more pronounced for n-pentane, which can be attributed to the energetically favorable all-*trans* conforma-

tion that n-pentane adopts in the crystalline phase [cf. Fig. 5(B)]. Also, the minimum of the potential energy lies at slightly larger density for the n-pentane crystal, and the $P_{IS}(\rho)$ curve of the n-pentane crystal is shifted towards higher densities with respect to the amorphous inherent structures. The uniform conformation in the crystal allows for a more efficient packing than in the amorphous phase. Close inspection of the ethane data reveals a similar, though much weaker trend. Note that the stress tensor which results from the isotropic expansion protocol used here reflects the anisotropy of the crystal structures. The pressures shown in Fig. 6 are obtained from the stress tensor $\boldsymbol{\sigma}$ as $P = -1/3 \operatorname{tr} \boldsymbol{\sigma}$.

Similar to the amorphous inherent structures, the crystals become unstable at low densities, and the systems fracture, leading to the appearance of large voids and a high-density solid phase. Initially, the crystal structure and symmetry are conserved upon isotropic expansion, the distance between the molecules increasing as $\rho^{-1/3}$ as the density is lowered. Interestingly, the density where the crystal becomes unstable [minimum in the $P_{IS}(\rho)$ curve] corresponds quite closely to the Sastry density ρ_S of the amorphous inherent structure in the case of ethane, whereas n-pentane crystals become unstable at noticeably higher density than the amorphous inherent structures. In both cases, the maximum tension that the crystals can sustain exceeds the isotropic tensile strength of
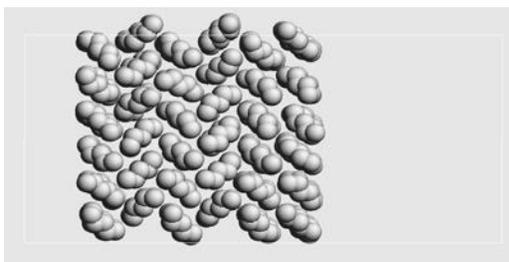
FIG. 7. United-atom n-pentane crystal after fracture. The system generates a new surface parallel to the $\langle 001 \rangle$ planes of the original crystals.

FIG. 8. (A) Fraction of end groups (CH_3 pseudoatoms) in the surface of the largest cavity present in n-pentane inherent structures. (B) Number of pseudoatoms (total and CH_3) in the surface of the largest cavity in n-pentane.

the amorphous inherent structures. Closer study of the n-pentane crystals around the instability point reveals that voids develop on $\langle 001 \rangle$ planes (cf. Fig. 7). These planes are not bridged by all-*trans* n-pentane molecules [cf. Fig. 5(B); the $\langle 001 \rangle$ planes correspond to vertical lines]. The cohesion between subsystems across $\langle 001 \rangle$ planes is entirely due to nonbonded intermolecular forces. Amorphous inherent structures, in contrast, do not contain such system-spanning weak links, which explains the greater density range of stability of the amorphous inherent structures. The much shorter ethane molecules do not seem to exhibit this ''reinforcement effect.'' Examination of the inherent structures obtained from n-pentane and ethane crystals at densities below the stability limit reveal that they consist of a continuous, system-spanning void phase, and of a crystalline phase with a large concentration of defects (cf. Fig. 7). This is in contrast to the complete amorphization which has been observed in a similar study on face-centered cubic (fcc) Lennard-Jones crystals by LaViolette.[5]

C. Chain-end segregation in n-pentane

Another goal of the present study was to establish the role that chain ends in linear molecules play in determining the stability limit of amorphous inherent structures subject to isotropic tension. Recently, an algorithm based on the Voronoi tesselation has been introduced by Sastry *et al.*[3] to rigorously detect and characterize voids in atomic structures. Each united atom unit is surrounded by an effective exclusion sphere of radius 3.92 Å (see Table I). The volume not occupied by exclusion spheres is the void volume. A cavity is a connected region belonging to the void volume. The algorithm identifies, for each cavity, the atoms which make up its surface. Using this information, the concentration of end groups (CH_3 pseudoatoms) in the cavity surfaces in n-pentane inherent structures is readily determined; results are shown in Fig. 8.

At high densities, the inherent structures are essentially homogeneous. In this case, the algorithm simply reports the largest Delaunay tetrahedron as the largest ''cavity'' in the structure. Therefore, the number of surface atoms [Fig. 8(B)] is equal to 4 in this range. At the Sastry density $\rho_S \approx 0.7$ g/cm³, the number of surface atoms increases sharply. The fraction of CH_3 pseudoatoms in the surface fluctuates around 0.6, significantly above the bulk average value of 0.4: the newly formed internal surfaces are highly enriched in end groups. This finding fits with the higher Sastry density ob-

served in the n-pentane crystals. Planes with a large concentration of end groups already exist in the crystal structure [cf. Fig. 5(B)] from the start and do not need to be nucleated upon expansion. Segregation of end groups to the surface of cavities has also been reported by Weber and Helfand[20] in their simulation study of spontaneous cavity formation in n-octane at finite temperature upon increasing the magnitude of the attractive intermolecular potential.
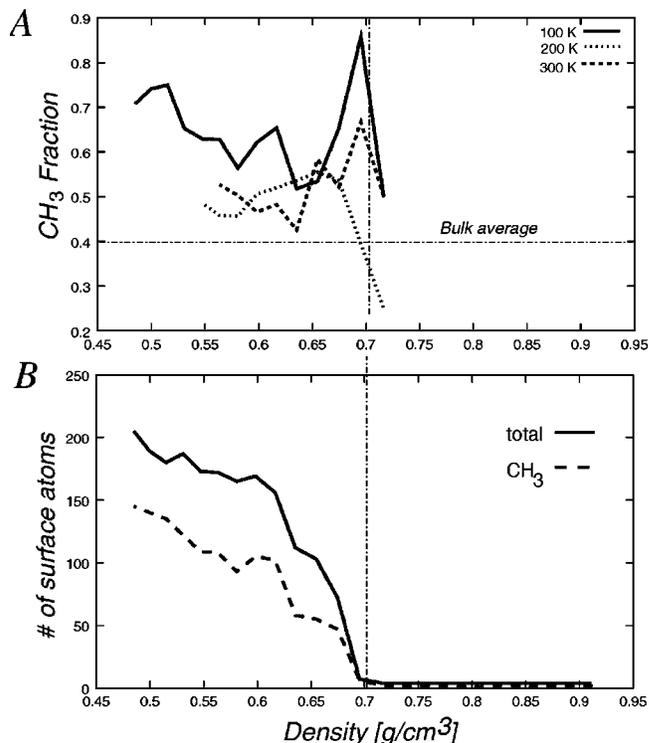
Notwithstanding the considerable scatter in the data, the results shown in Fig. 8 suggest that the enrichment of CH_3 pseudoatoms is more accentuated in structures generated at lower equilibration temperatures, probably because the n-pentane molecules tend towards more elongated conformations at low temperature.

IV. CONCLUSIONS

The density dependence of the energy landscape of three simple alkanes, ethane, n-pentane, and cyclopentane, has been explored using a united-atom representation. Investigation of the relationship between inherent structure pressure and density $P_{IS}(r)$ provides information on the isotropic tensile strength of glasses of these materials. Pronounced variation of the inherent structure energy with the equilibration temperature of the liquid was observed for the conformationally flexible n-pentane, whereas the inherent structures in the other systems exhibited considerably less temperature dependence. In all three cases, the equation of state of the energy landscape was nearly unaffected by the equilibration temperature. The complex behavior of n-pentane's inherent

structure energy is due to the temperature dependence of the distribution of conformers in the liquid, which is essentially conserved upon steepest descent minimization. On account of the rather different shapes and packing geometries expected for n-alkanes containing *trans*-to-*gauche* twists compared to all-*trans* conformers, the near invariance with respect to temperature of amorphous deposit maximum tensile strength and limiting (Sastry) density observed for n-pentane is a somewhat surprising outcome of the present investigation. An attractive opportunity now exists for future studies to examine whether this invariance with respect to equilibration temperature extends to substantially longer-chain n-alkanes.

Interestingly, the n-pentane example raises related questions about other forms of molecular complexity, and whether the correspondingly complex energy landscapes probed by varying equilibration temperature are similarly decoupled from the strength of the substances' amorphous deposits. In this respect, we suggest that it would be profitable to focus both experimental and theoretical attention on systems whose liquid structures depend strongly on temperature. Specific examples would include block copolymer melts, and binary mixtures close to a phase separation point (upper or lower consolute point). It has recently been shown that the isochoric dependence of inherent structure energy upon the equilibration temperature provides information on supercooled liquid dynamics.[1] The present results, therefore, raise interesting questions regarding the relationship (or lack thereof) between liquid-phase dynamics and the mechanical properties of the corresponding glasses.

Crystalline inherent structures of ethane and n-pentane, generated from experimental data and used in the present study, show higher isotropic tensile strength than their amorphous counterparts. In the case of n-pentane, the range of densities over which the system can sustain tension without fracturing is narrower for the crystal than for the amorphous inherent structures. It is not clear at present which molecular attributes are important for this narrowing effect, especially in light of the fact that the isotropic tensile strength of all three amorphous systems studied was very similar. The very insensitivity of the ultimate tensile strength of these three materials to details of molecular architecture is surprising as well, and prompts inquiry into the general problem of understanding, from a molecular perspective, the strength of materials when placed under tension. We conclude that further examinations involving substantially longer and/or branched molecules will be necessary to resolve these interesting questions.

The voids formed in the n-pentane simulations upon expansion below the limiting (Sastry) density were found to be significantly enriched in end groups. This effect was most pronounced just below that mechanical-stability density limit, where the overall size of the internal surface is yet small, suggesting strongly that local regions of anomalously high end-group concentration constitute "weak spots" in the medium.[4] This viewpoint is reinforced by our observation that the n-pentane crystals fracture along planes at which end groups accumulate. The mechanical fracture phenomenon for amorphous media investigated herein amounts to an absolute-zero-temperature cavitation event. It is therefore reasonable to postulate that positive-temperature cavitation and bubble nucleation events in linear-alkane liquids might also initiate preferentially at weak spots created by local end-group concentrations.

In the event that only repulsive intermolecular forces were present, the system pressure would be restricted to non-negative values. Careful examination at least of simple models of this sort[7] reveals that at every attainable pressure, there exist isothermal pairs of fluid and crystal phase densities for which the molar entropies are identical. These equal-entropy pairs define a "Kauzmann curve" in the (ρ, P) plane, so-called because of the historical connection to the "Kauzmann paradox."[8] With attractive forces present as well, both fluid (i.e., amorphous) and crystalline phases can (metastably) penetrate into the negative pressure, or isotropic tension, regime. As a result, the Kauzmann curve similarly must possess extension to negative pressure, terminating finally at that most negative pressure which can be sustained simultaneously by both phases. The alkane results reported above agree with a previous mean-field approximate analysis,[7] to the effect that the weaker amorphous phase at the limiting (Sastry) density sets the lower limit on P, not the crystal. Consequently, the Kauzmann curve for those cases examined so far necessarily terminates at the point of maximum mechanical strength for the amorphous deposits, i.e., at the inherent structure Sastry point. It is not inconceivable that the relative mechanical strengths of amorphous and of crystal phases might be reversed for some anomalous substances, but for the present this possibility must remain an open question.

ACKNOWLEDGMENTS

[1] S. Sastry, P. G. Debenedetti, and F. H. Stillinger, Nature (London) **393**, 554 (1998).
[2] F. H. Stillinger, Science **267**, 1935 (1995).
[3] S. Sastry, D. S. Corti, P. G. Debenedetti, and F. H. Stillinger, Phys. Rev. E **56**, 5524 (1997).
[4] S. Sastry, P. G. Debenedetti, and F. H. Stillinger, Phys. Rev. E **56**, 5533 (1997).
[5] R. A. LaViolette, Phys. Rev. B **40**, 9952 (1989).
[6] The appearance of voids in the inherent structure is not directly related to the phenomenon of cavitation of the liquid under tension. Negative pressures can occur in the inherent structure even when the corresponding liquid (at finite temperature) is still in a state of positive pressure.
[7] P. G. Debenedetti, F. H. Stillinger, T. M. Truskett, and C. J. Roberts, J. Phys. Chem. B **103**, 7390 (1999).
[8] W. Kauzmann, Chem. Rev. **43**, 219 (1948).
[9] J. H. Gibbs and E. A. DiMarzio, J. Chem. Phys. **28**, 373 (1958).
[10] F. H. Stillinger, J. Chem. Phys. **88**, 7818 (1988).
[11] C. J. Roberts, P. G. Debenedetti, and F. H. Stillinger, J. Phys. Chem. B **103**, 10258 (1999).
[12] B. Smit, S. Karaborni, and J. I. Siepmann, J. Chem. Phys. **102**, 2126 (1995).
[13] B. Smit, S. Karaborni, and J. I. Siepmann, J. Chem. Phys. **109**, 352 (1998).
[14] M. P. Allen and D. J. Tildesley, *Computer Simulation of Liquids* (Clarendon, Oxford, 1987).

[15] D. Rigby and R.-J. Roe, J. Chem. Phys. **87**, 7285 (1987).
[16] W. H. Press, S. A. Teukolsky, W. T. Vetterling, and B. P. Flannery, *Numerical Recipes in C*, 2nd ed. (Cambridge University Press, Cambridge, 1992).
[17] D. Y. Peng and D. B. Robinson, Ind. Eng. Chem. Fundam. **15**, 59 (1976).

[18] G. J. H. van Nes and A. Vos, Acta Crystallogr., Sect. B: Struct. Crystallogr. Cryst. Chem. **B34**, 1947 (1978).
[19] H. Mathisen, N. Norman, and B. F. Pedersen, Acta Chem. Scand. **21**, 127 (1967).
[20] T. A. Weber and E. Helfand, J. Chem. Phys. **72**, 4014 (1980).